

PAPER • OPEN ACCESS

## Stirring flow of liquid metal generating by low-frequency modulated traveling magnetic field in rectangular cell

To cite this article: G Losev *et al* 2019 *IOP Conf. Ser.: Mater. Sci. Eng.* **581** 012005

View the [article online](#) for updates and enhancements.

**ECS**  
The Electrochemical Society  
THE KOREAN ELECTROCHEMICAL SOCIETY

**The best technical content in  
electrochemistry and solid state  
science and technology!**

**Available until November 9, 2020.**

**PRIME™**  
PACIFIC RIM MEETING  
ON ELECTROCHEMICAL  
AND SOLID STATE SCIENCE  
**2020**

**REGISTER TO ACCESS  
CONTENT FOR FREE! ▶**

# Stirring flow of liquid metal generating by low-frequency modulated traveling magnetic field in rectangular cell

G Losev<sup>1</sup>, A Pavlinov<sup>1</sup>, E Shvydkiy<sup>2</sup>, I Sokolov<sup>2</sup>, I Kolesnichenko<sup>1</sup>

<sup>1</sup> Institute of Continuous Media Mechanics of the Ural Branch, RAS, Perm, Russia

<sup>2</sup> Ural Federal University, Yekaterinburg, Russia

E-mail: Losev.g@icmm.ru, PAM@icmm.ru, E.L.Shvydky@urfu.ru, I.V.Sokolov@urfu.ru, KIV@icmm.ru

**Abstract.** In the present work the influence of low frequency modulation of a travelling magnetic field (TMF) on a process of generation of electro-vortex flows in electrically conducting media are numerically and experimentally investigated. The measurements are carried out on a low melting temperature GaZnSn alloy by means of Ultrasonic Doppler Velocimetry. For numerical simulation, Comsol Multiphysics software was used. The dependencies of average and pulsating Reynolds numbers on the magnitude of electromagnetic impact and two modes of low frequency modulation are considered. A positive influence of reversed TMF modulations on the stirring process is determined. In particular the formation of a small-scale vortex structure in the main volume of liquid media.

## 1. Introduction

The metal production and development of alloys with specific properties is one of the great challenges of modern metallurgy. The stirring of metals during the crystallization process allows to improve the quality of ingots, homogenization of the impurity distribution and metal grain grinding [1–3].

Due to the high temperature and chemical activity of most liquid metals and salts, electromagnetic processing proved to be useful. The method of electromagnetic excitation of flows can be readily applied without contact with a conductive medium. Thereby, the contactless generation and control of flows is applicable in the field of non-ferrous and ferrous metals preparation.

In the conductive medium the alternating magnetic field excite eddy currents. The interaction of these currents with the initial magnetic field leads to the generation of an electromagnetic force. In the case of liquid medium, the force generates vortex flows. Such flows increase the intensity of heat transfer and exchange in the melts [4], smooth the crystallization front [5] and increase the energy efficiency of operations [6]. Electromagnetic stirring by rotating and travelling magnetic fields (TMF) during the crystallization of ingots is widely used [7].

In a recent time a several works are dedicated to study of influence of the TMF characteristics on a liquid metal flow and solidification process. Wang et al. [8,9] analytically and experimentally described the behavior of liquid metal flow under the reversed TMF. The parametric study is shown that flow velocity has a saturation zones and authors suggest optimal modulation period



criteria. Than Hachani et al. [5,10] experimentally approved that modulating of TMF can have a positive affect on a the solidification macrostructure and the segregation behavior. Musaeva et al. [11] experimentally shown the influence of pulsating TMF on a solidification front shape smoothing. Avnain et al. [4,12] made a numerical and experimental study of liquid metal flow and solidification parameters under the steady applied TMF impact. All of the above mentioned works notice that modulation of TMF has a positive effect on a stirring process efficiency. Additionally the low-frequency modulation of the magnetic field can potentially reduce metal processing energy costs due to the appearance of a power supply off-period. However the question of influences of TMF inductor parameters such as transverse longitudinal end effect, and the penetration depth of the magnetic field into the metal on a flow structure is still open.

This paper is dedicated to the experimental and numerical model of liquid metal stirring process under the external controlled travelling magnetic field (TMF). The goal of the present work is to obtain the flow characteristics under the control the stirring efficiency by low-frequency modulation of the TMF. The geometry of the working cavity is consistent with the geometry of casting machines. The results obtained could be applied in the field of improving the quality of ingots and moldings in-process and in finished products. The verification of the proposed numerical algorithm allows it to be applied to channels and cavities of an arbitrary geometry and stirring regimes.

## 2. Experimental setup

The experimental setup (Fig. 2) consists of a vertical cell 1 made from plexiglass. The cell is filled with liquid GaSnZn alloy. The alloy's physical properties at the working temperature are density  $6256 \text{ kg/m}^3$ , kinematic viscosity  $3 \cdot 10^{-7} \text{ m}^2/\text{s}$ , and conductivity  $3.56 \cdot 10^6 \text{ Sm}$ . The top surface of the metal was covered by a thick layer of mineral oil to prevent the oxidation of the melt. The cell measures  $450 \times 20 \times 75 \text{ mm}^3$ . The channel was placed on a linear inductor of the TMF 2 with dimensions of  $480 \times 350 \text{ mm}^2$ . The TMF was generated by six coils with a winding of 170 turns. The coils were fed from a three-phase programmable Pacific Smart Source 360 ASX-UPC3 3. This power supply unit made it possible to specify the shape of the output signal and to modulate the TMF. The main frequency of the current supply (and so the TMF) was 50 Hz. The modulation frequency was in the range  $0.02 - 0.1 \text{ Hz}$ .

The liquid metal flow velocity was measured by an ultrasonic Doppler velocimeter 4 (UDV) DOP 2000, Signal Processing. Four sensors 5 of the UDV were placed on the thin wall of the cell. The UDV method involves emission of ultrasound wave packets by an ultrasonic transducer, reception of reflected pulses (echoes) and calculation of the Doppler frequency shift between the emitted and received wave packets. The presence of sound-reflecting particles driven by the flow in the liquid medium is also necessary. The gallium oxide particles were used to reflect the ultrasound waves in the gallium eutectic. These particles were formed by the oxidation of gallium in the atmosphere [13].

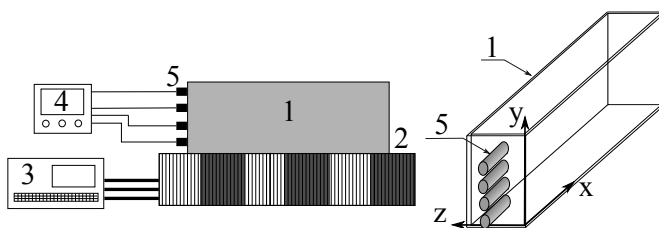


**Figure 1.** Experimental setup: 1. cell with liquid metal, 2. LIM, 3. power supply, 4. UDV, 5. UDV traducers.

### 3. Numerical model

The 3D numerical calculations were carried out by the finite element method using the Comsol Multiphysics software. At the first stage for electromagnetic calculations we used the Maxwell equations, which were formulated in terms of the magnetic vector potential. The calculations of the magnetic field, induced current and Lorentz force distribution were made with the use of the Magnetic Fields interface. Under the assumption of low magnetic Reynolds number ( $Re_m = 0.065$ ), the induced current density was calculated by noninductive formulation [1,14,15].

The phase shift of inductor windings was  $60^\circ$  and the supplied current was in the range of 1 to 18 A. Analysis of magnetic saturation showed that the magnetic core saturates at 25 A and more [16], so the magnetic permeability has a constant value of  $\mu = 150$ . The LIM coils were modeled by a homogenized multi-turn coil, whose winding consisted of 170 turns of copper wire. The mesh for electromagnetic calculation included 152329 tetrahedral, 16246 triangular and 13200 hexahedral elements. The mesh for the cell domain was built using rectangular elements. Refinement of the mesh is performed toward the bottom layer of the domain taking into account the skin effect.

The electromagnetic force acting on a liquid metal was calculated as the product of current density and magnetic induction. Then the resulting electromagnetic force field was transferred to the hydrodynamic part as a source term of the Navier-Stokes equation. Hydrodynamic flow was calculated only in the liquid metal domain which is placed on a TMF inductor. The maximum Reynolds number was  $Re = 1.5 \cdot 10^4$ , therefore melt flow is described by the  $k-\omega$  SST turbulent model. We prescribed the slipping condition at the boundary of the top surface and the no-slip condition at the remaining walls. The computational domain contained 37500 hexahedral and 7750 quadrilateral finite elements. The maximum element size was limited to 5 mm and the mesh was refined at the domain boundaries areas.

### 4. Results

In the course of the work, measurements of the flow velocity profiles along the cell were made. The velocity characteristics were the main criterion for determining the quality of the mixing of the liquid metal. Fig. 2 demonstrates time-averaged velocity profiles. As can be seen, the flow has a two-vortex structure. The larger vortex occupies the central region of the cell. At the same time, a smaller vortex is formed in the near-wall region (Fig. 2a, c). Its formation is associated with the influx of fluid to the wall and the curvature of the streamlines. The rate of this vortex is slightly higher than the rate of the central vortex. With an increase in the external influence intensity, the energy of the vortices increases, which leads to a distortion of the free metal boundary in the region of the vortices localization.

The greatest velocity flow rate is near the bottom boundary of the cell in the region adjoining the TMF inductor (Fig. 2a). In the same area, the largest amplitude of velocity pulsations are observed. The velocity pulsation amplitude maximum is observed in the first third of the layer along its length. The pulsation magnitude varies slightly both in the height and in the length of the cell.

The imposition of low-frequency modulations on the TMF results in the restructuring of the flow pattern. The described average profiles undergo a qualitative change: the average component of the flow decreases (up to complete disappearance with small period reverse modulations), while the pulsating component tends to repeat the velocity distribution characteristic of the unmodulated force action. Fig. 3 represents the typical velocity time series in the median of the velocity profile. The imposition of low-frequency pulsations on the external electromagnetic force naturally leads to a periodicity in the generation of the flow. The frequency of the emerging hydrodynamic structures coincides with the modulation frequency of the TMF, and the magnitude of the flow velocity coincides with the magnitude of the average flow in the absence of modulations. Velocity oscillation occurs around a non-zero mean value with a periodic

decrease in the velocity rate of large-scale flow to zero. In the reverse modulation mode, the velocity oscillations occur near zero mean value and the large-scale flow changes its direction with the TMF modulation frequency. High-frequency hydrodynamic pulsations are observed on the background of both average flow and large-scale low-frequency-modulated flow.

As the main characteristics for the stirring efficiency of a liquid metal, the mean  $Re_m$  and the pulsation  $Re_p$  Reynolds numbers calculated for the maximum on the average and pulsating velocity x-components were chosen. Fig. 4 represents the dependencies of Reynolds numbers on the intensity of electromagnetic field intensity and the TMF modulation period.

As the intensity of the external influence increases, the flow velocity increases nonlinearly with the release into the YsaturationY region at inductor supply currents of more than 6 A. In this case, both the average and pulsation Reynolds numbers reach the maximum (Fig. 4a, b). The results of numerical simulation correspond well with the experimental data. A difference is only observed near the upper surface of the metal due to the curvature of the free surface in the experiment, which is not taken into account in the numerical model. The best convergence of numerical and experimental data is provided at low values of the current in the coils due to the weak influence of the flow on the shape of the free surface. The maximum attainable average Reynolds number only slightly exceeds the pulsation Reynolds number maximum, which indicates a significant contribution of small-scale flows to the overall flow structure. Nevertheless, the presence of the YsaturationY region shows the ineffectiveness of controlling the mixing of the liquid metal only by a increasing in the power pumped into the system alone. This leads to

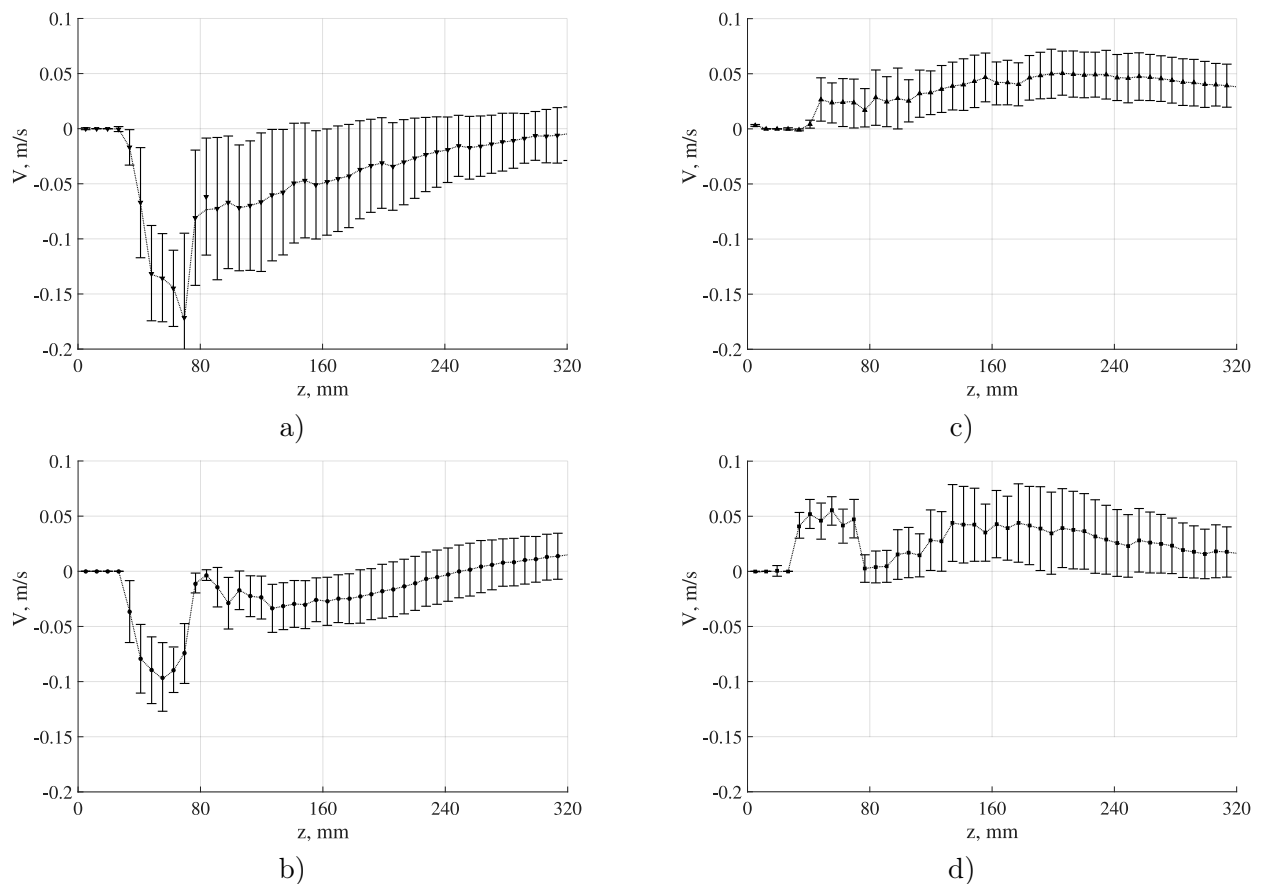


**Figure 2.** Time average velocity profiles on several levels of the cell: a) 14 mm, b) 30 mm, c) 46 mm, d) 62 mm. The errorbars represent amplitude of velocity pulsations.

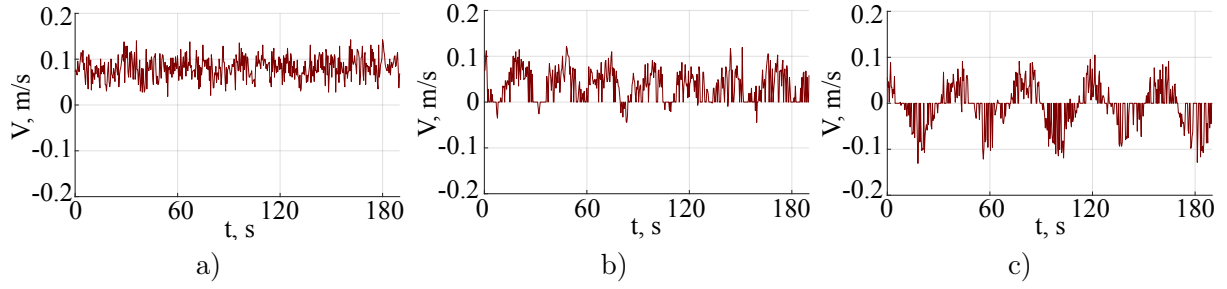


**Figure 3.** Velocity time series in three cases of external action: a) TMF without modulation, b) modulated TMF, c) reverse modulation TMF. Modulation period  $\tau = 30$  s in both modulation cases.

the need to develop additional mechanisms for introducing small-scale hydrodynamic structures into the main flow. The modulation of electromagnetic exposure can serve as such a mechanism

The modulated flow was created at the amplitude of the supply current of 6.0 A. Thus, the condition of minimizing energy consumption with a maximum increase in the rate of metal flow was fulfilled. In the modulation mode, the amplitude of the TMF changed according to a periodic law from zero to amplitude with a period  $\tau = 5 - 50$  s. The dependences of the mean and pulsation Reynolds numbers are given in Fig. 4c, d. As the modulation period increases, the  $Re_m$  decreases. At the same time, there is an assignment increase of  $Re_p$ . The greatest intensity of hydrodynamic pulsations is observed in the region of the localization of a large-scale vortex (near the bottom of the cell and the free surface). These pulsations repeat the form of the electromagnetic effect and are a low-frequency quasi-stationary flow against the background

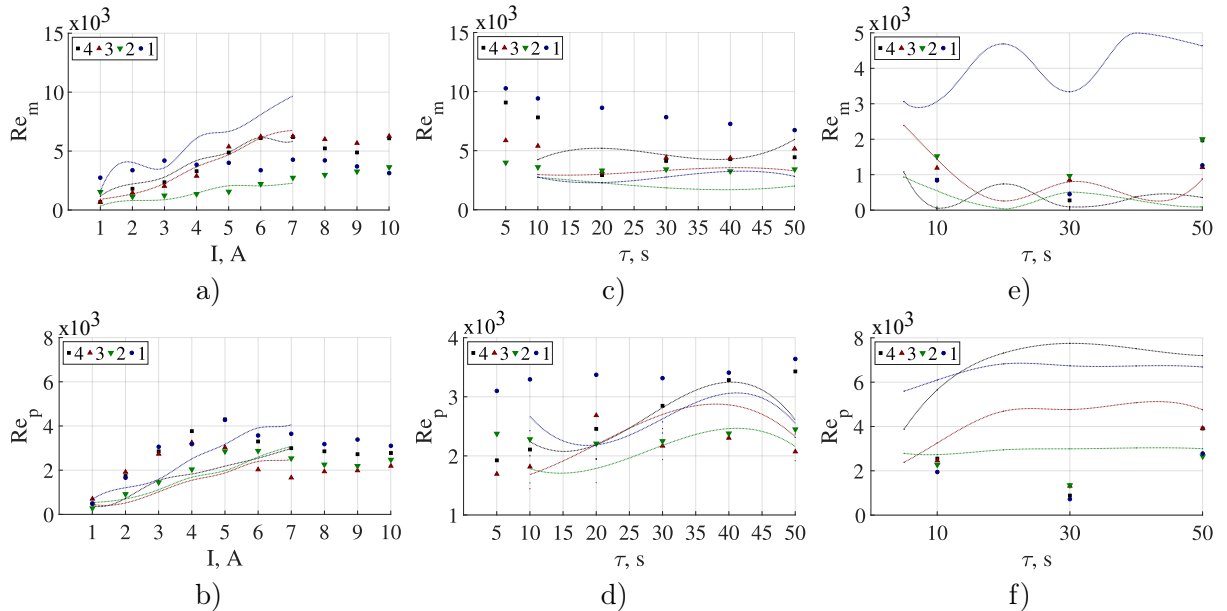


**Figure 4.** Time average flow velocity (a, c, e) and amplitude of velocity pulsation (b, d, f) vs supply current (a, b), period of MVT modulation (c, d) and period of reverse modulation (e, f). The line represents numerical results and the points represents experimental data. The numbers in the legend represent heights of lower cross-sections: 1) 62 mm, 2) 46 mm, 3) 30 mm, 4) 14 mm

of which secondary small-scale structures arise.

The second considered modulation mode of the TMF we will call reverse. In this case, the magnitude of the magnetic induction varied over the period according to the sinusoidal law. In the second half-cycle, the direction of the TMF was changed. This reverse modulation generated a pronounced pulsed flow in the liquid phase. The reverse flow pattern is characterized by low values of  $Re_m$  due to the periodic change of direction of large-scale eddies. The significant difference between the experimental and numerical data in the region of the upper surface of the metal is explained by the change in the shape of the free surface with a periodic change in the direction of large-scale vortex structures rotation. However, in the main volume of the cuvette, experimental data and simulations are consistent.

The pulsating component of the reverse flow has a peculiarity as significant contribution of small-scale (in the sense of the spatial dimensions and turnover periods of the vortex ) to the overall structure of the flow compared to the previously considered modes. Due to the limited resolution of the spatial and temporal scales of the vortex structures of UDV, the experimentally obtained values of  $Re_p$  are underestimated in comparison with the numerical simulation that resolves much smaller scale structures. Based on the simulation data (in the layer main volume), we can conclude about the double increasing of  $Re_p$  in the case of low-frequency reverse modulation compared with the cases of no flow modulation or amplitude modulation.

## 5. Conclusions

In the course of the work, the characteristics of the liquid metal vortex flow generated by the external action of TMF under the action of low-frequency modulations have been investigated. The flow characteristics and structure were found experimentally and numerically.

Under the action of steady applied TMF, the two-vortex flow appears in the metal. The intensity of the vortices grown nonlinearly and has the «saturation» region at supply coil current more than 6 A. The formation of a large-scale vortex with an intensity independent of the magnitude of the applied electromagnetic effect could have a negative impact on the distribution of impurities and alloying additives in the volume of the metal due to the retention of impurities by the vortex. The presence of the maximum flow rate limit leads to the need to introduce new mechanisms to improve the efficiency of mixing. In this way, the control of the induction machine power supply can be a solution. The obvious advantage of the method is its technical simplicity and the cheapness of modifying existing technological installations.

The low-frequency modulation of the LIM supply increases the intensity of small-scale flows generated in the volume of the mixed melt. This also has a positive effect on the heat transfer during the crystallization of castings (smoothes the crystallization front and reduces the number of grain effects). Changing the direction of TMF destroys large-scale eddies and creates multiple small-scale flows that promote efficient mixing of the medium. This LIM power mode can be achieved using the simple relay contactor circuit.

The limited capabilities of existing experimental techniques lead to the need for the development and verification of numerical models that take into account the specifics of individual tasks (including cavity geometry, mutual influence of electromagnetic fields of all installation sites, phase transformations). In this paper, an attempt to advance in the field of numerical simulation and verification of the MHD model has been made. Despite some imperfections the used model allows one to adequately describe the structure and characteristics of the flow in the main volume of the liquid metal.

## Acknowledgments

The work of Institute of Continuous Media Mechanics team is supported by the RFBR grant 17-48-590539\_r\_a and the work of Ural Federal University team is supported by Act 211 Government of the Russian Federation, contract e 02.A03.21.0006.

## References

- [1] Denisov S, Dolgikh V and Khripchenko S 2014 *Magnetohydrodynamics* **4** 249 – 265
- [2] Eckert S, Nikrityuk P A, Willers B, Rübiger D, Shevchenko N, Neumann-Heyme H, Travnikov V, Odenbach S, Voigt A and Eckert K 2013 *The European Physical Journal Special Topics* **220** 123–137 ISSN 1951-6401 URL <https://doi.org/10.1140/epjst/e2013-01802-7>
- [3] Garrido M, Davoust L, Daudin R, Salvo L and Fautrelle Y 2018 *IOP Conference Series: Materials Science and Engineering* **424** 012001 URL
- [4] Avnaim M, Mikhailovich B, Azulay A and Levy A 2018 *International Journal of Heat and Fluid Flow* **69** 23 – 32 ISSN 0142-727X URL <http://www.sciencedirect.com/science/article/pii/S0142727X17302874>
- [5] Hachani L, Zaidat K and Fautrelle Y 2015 *International Journal of Heat and Mass Transfer* **85** 438 – 454 ISSN 0017-9310 URL <http://www.sciencedirect.com/science/article/pii/S0017931015001660>
- [6] Fdhila R, Sand J U, Eriksson E and Yang H 2016 *ABB Review* **3**
- [7] Moffatt H K 1991 *Phys. Fluids A* **3** 1336–1343
- [8] Wang X, Moreau R, Etay J and Fautrelle Y 2008 *Metall. Mater. Trans. B* **40** 82 URL <https://doi.org/10.1007/s11663-008-9176-0>
- [9] Wang X, Moreau R, Etay J and Fautrelle Y 2009 *Metall. Mater. Trans. B* **40** 104–113 URL <https://link.springer.com/article/10.1007/s11663-008-...>
- [10] Zaidat K, Sari I, Boumaaza A, Abdelhakem A, Hachani L and Fautrelle Y 2018 *IOP Conference Series: Materials Science and Engineering* **424** 012052 URL <https://doi.org/10.1088/1757-899X/424/1/012052>
- [11] Musaeva D, Baake E, Köppen A and Vontobel P 2017 *Magnetohydrodynamics* **53** 583–593 ISSN 0024998X
- [12] Avnaim M, Mikhailovich B, Azulay A and Levy A 2018 *International Journal of Heat and Fluid Flow* **69** 9 – 22 ISSN 0142-727X URL <http://www.sciencedirect.com/science/article/pii/S0142727X17302886>
- [13] Nowak M 2002 *Experiment in fluids* **31** 249 – 255
- [14] Branover G and Cinober A 1970 *Magnetohydrodynamics of incompressible medium* (M.: Science)
- [15] Kolesnichenko I, Khalilov R, Khripchenko S and Pavlinov A 2012 *Magnetohydrodynamics* **1** 221 Ч 234
- [16] Shvydkiy E and Kolesnichenko I 2018 3D numerical simulation of the linear induction motor, considering magnetic saturation *2018 IEEE Conference of Russian Young Researchers in Electrical and Electronic Engineering (EIConRus)* pp 777–779